Pinned magnetization in the antiferromagnet and ferromagnet of an exchange bias system

M. R. Fitzsimmons,[1] B. J. Kirby,[1] S. Roy,[2] Zhi-Pan Li,[2] Igor V. Roshchin,[2] S. K. Sinha,[1,2] and Ivan K. Schuller[2]
[1]*Los Alamos National Laboratory, Los Alamos, New Mexico 87545, USA*
[2]*Department of Physics, University of California at San Diego, La Jolla, California 92093, USA*
(Received 24 December 2006; revised manuscript received 13 March 2007; published 6 June 2007)

Using polarized neutron reflectometry, we obtained separate depth profiles for *pinned* and *unpinned* magnetization across the interface of a ferromagnet/antiferromagnet bilayer as a function of the sign of exchange bias. The *pinned* and *unpinned* magnetization depth profiles are nonuniform and extend well beyond the chemical interface, suggesting an interfacial region magnetically distinct from its surroundings. A model that includes *pinned* and *unpinned* moments in the ferromagnet and antiferromagnet is developed for a complete description of the data.

DOI: 10.1103/PhysRevB.75.214412 PACS number(s): 75.70.Ak, 75.70.Cn, 61.12.−q

I. INTRODUCTION

The magnetization (M) of a ferromagnet (FM) can be *pinned* through exchange coupling with an antiferromagnet (AF). The magnetization (or moment) is *pinned* (M^P) if it does not respond to modest fields (tens of kilo-oersted). A manifestation of exchange coupling between *unpinned* and *pinned* moments is the shift of the ferromagnetic hysteresis loop along the field axis—a phenomenon called exchange bias.[1–5] The sign of exchange bias, positive or negative, refers to the shift of the loop with respect to the cooling field H_{FC}. H_{FC} is the field applied to the sample as it is cooled through the Néel temperature T_N of the AF. If the loop is shifted in the direction opposite to H_{FC}, then exchange bias is negative, $-H_E$.[6] Many FM/AF systems exhibit $-H_E$. However, some systems containing FeF_2, $(Zn,Fe)F_2$, or MnF_2,[6,7] or magnetic oxides, e.g., $La_{0.67}Sr_{0.33}MnO_3/SrRuO_3$,[8] and ferromagnetic systems, e.g., FeSn/FeGd,[9] exhibit positive exchange bias, $+H_E$. The sign of exchange bias can be influenced by environmental variables such as cooling field[7] and temperature[10,11] or by changes of the domain state[12] in the AF bulk or at the FM/AF interface.[10,13] $+H_E$ is commonly thought to arise from antiferromagnetic exchange coupling between *unpinned* moments in the FM and *pinned* uncompensated moments in the AF.[6–9] Antiferromagnetic exchange coupling favors opposite (antiparallel) alignment of the *unpinned* and *pinned* moments, while ferromagnetic exchange coupling favors the same (parallel) alignment. An early model explaining the sign of exchange bias,[6] considered two layers: the uncompensated *pinned* spins in the AF couple antiferromagnetically to *unpinned* spins in the FM. The sign of H_E was determined through the competition between the exchange coupling across the interface with the Zeeman interaction of the uncompensated AF spins with H_{FC}. For weak H_{FC}, antiferromagnetic coupling (across the FM/AF interface) prevailed, and the uncompensated moments in the AF were oriented and subsequently frozen in the direction opposite to H_{FC}. This resulted in $-H_E$. For large H_{FC}, the Zeeman interaction between the field and the uncompensated moments in the AF overcame the exchange coupling across the FM/AF interface and aligned the uncompensated AF moments parallel to H_{FC}, leading to $+H_E$ after cooling. The early model assumed that all uncompensated AF moments were located immediately at the FM/AF interface, and no depth dependence was considered. Further, the model assumed that all the FM moments were *unpinned*.

By identifying where the magnetization is *pinned* and the alignment of the *unpinned* magnetization with respect to the *pinned* magnetization as a function of field, the sign of exchange coupling, either ferromagnetic or antiferromagnetic, can be inferred. Key to understanding the origin of exchange bias is the measurement of *pinned* and *unpinned* magnetization depth profiles. Since the net magnetization of an ideal AF at zero field is zero, net magnetization in an AF refers to the *uncompensated* magnetization[14] of a nonideal AF, which may also result from proximity to a FM.

Previously, Nogués *et al.*[7] correlated exchange bias with *pinned* magnetization in Fe/FeF_2 and Fe/MnF_2 bilayers with twinned AF layers using a superconducting quantum interference device (SQUID) magnetometer.[7] In their experiment, exchange bias was varied by changing the growth conditions of the samples or the strength of H_{FC}. The *pinned* magnetization was obtained from *vertical* shifts of the hysteresis loops. For instance, an upward shift was related to a net *pinned* magnetization parallel to H_{FC}. Ferromagnetic exchange coupling across the interface gave rise to an upward shift for all cooling fields with a minor change of exchange bias. In contrast, antiferromagnetic coupling led to a downward shift for small cooling fields. Thus, the sign of interfacial exchange coupling could be inferred from magnetometry, provided the *pinned* magnetization is *confined* in the AF close to the FM/AF interface. In particular, the *pinned* magnetization in the AF bulk must be negligibly small in comparison to the *pinned* interfacial magnetization.

Since the *pinned* magnetization of the AF cannot be distinguished from *pinned* interfacial magnetization with magnetometry, we previously measured the magnetization depth profile of an exchange bias system [Co/FeF_2 (untwinned)] using polarized x ray and neutron scattering.[15] This study identified significant *pinned* magnetization in the AF bulk and showed that *unpinned* Fe moments *beneath* the Co/FeF_2 interface were antiparallel to *unpinned* Co moments above the interface. However, since neither x ray nor neutron-scattering measurements were taken in saturating fields applied in opposite directions and with *both* polarizations of the incident neutron (or x-ray) beam, the magnetization depth profiles could not be separated into *pinned* and *unpinned*

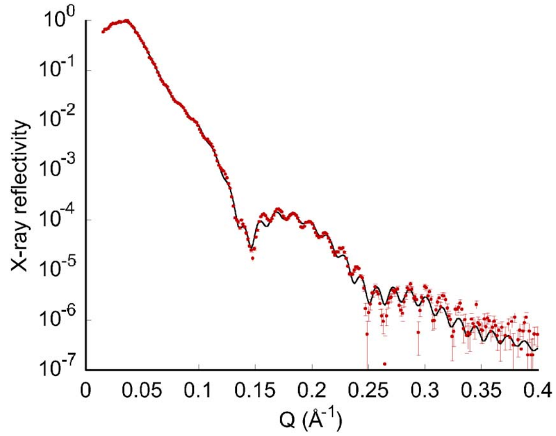

FIG. 1. (Color online) The x-ray reflectivity of the sample: observed (○) and calculated (solid curve) from the model structure (Fig. 2).

components. Consequently, the previous study left unresolved the depth profile of the *pinned* magnetization across the Co/FeF_2 interface–a key issue in exchange bias.

Here, we report new neutron-scattering data that allow us to separate the magnetization depth profile into *pinned* and *unpinned* components with nanometer spatial resolution. We investigated a sample with exchange bias that could be switched from negative to positive just by cooling in weak or strong magnetic fields.[13] This study yields insight into the sign of exchange coupling that gives rise to H_E. Our observations motivate an exchange bias model with *pinned* magnetization not only in the AF as commonly assumed, but in the FM as well. Our model consistently explains the x-ray and neutron-scattering data.

II. SAMPLE PREPARATION

Exchange bias samples were prepared by sequential electron-beam evaporation of FeF_2, Co, and Al at a deposition rate of 0.05 nm/s onto (110) oriented single-crystal MgF_2 polished substrates measuring 10×10 mm^2. The deposition temperatures were 300 °C for the FeF_2 layer and 150 °C for the Co and Al layers. The chemical depth profile of the sample was determined from x-ray reflectometry.[16] The x-ray reflectivity is shown in Fig. 1 as a function of wave-vector transfer $\vec{Q}=\vec{k}_f-\vec{k}_i$, where $\vec{k}_f$ and $\vec{k}_i$ represent the final and incident wave vectors, respectively. Layer thickness and interface roughness are reported in Fig. 2. In-plane glancing angle x-ray diffraction (not shown) confirmed that the AF layer was an untwinned single-crystal film with $[1\bar{1}0]FeF_2\|[1\bar{1}0]MgF_2$. X-ray diffraction also indicates that the Co film is polycrystalline.[13] A uniaxial magnetic anisotropy is present in the Co film with its easy axis along the FeF_2 easy axis, even for temperatures much higher than T_N—a property attributed to growth-induced anisotropy.[13]

To promote $+H_E$, a field of 7 kOe was applied along [001] FeF_2 at room temperature, and then the sample was cooled to 10 K. To promote $-H_E$, the sample was cooled from 300 to 150 K in a field of 7 kOe (applied along [001] FeF_2), and then the sample was cooled to 10 K in a field of 100 Oe.[17] The hysteresis loops measured with a SQUID magnetometer are shown in Fig. 3. The magnitude of H_E was 2.2 kOe, regardless of the sign of exchange bias. For cooling field strengths intermediate between those we have chosen, the magnetization curves consists of two loops—one centered at $-H_E$ and the other centered at $+H_E$.[13] As H_{FC} is increased or decreased, one loop grows at the expense of the other.[13] For H_{FC}=7 kOe, a loop centered at $-H_E$ is mostly suppressed. Only about 4% of this loop remains as evidenced by the small (positive) increase in the magnetization (closed symbols, Fig. 3) near remanence. For H_{FC}=100 Oe, a loop centered at $+H_E$ is completely suppressed.

III. MEASUREMENTS AND RESULTS

The magnetization depth profiles were obtained using polarized neutron reflectometry with polarization analysis.[18–20]

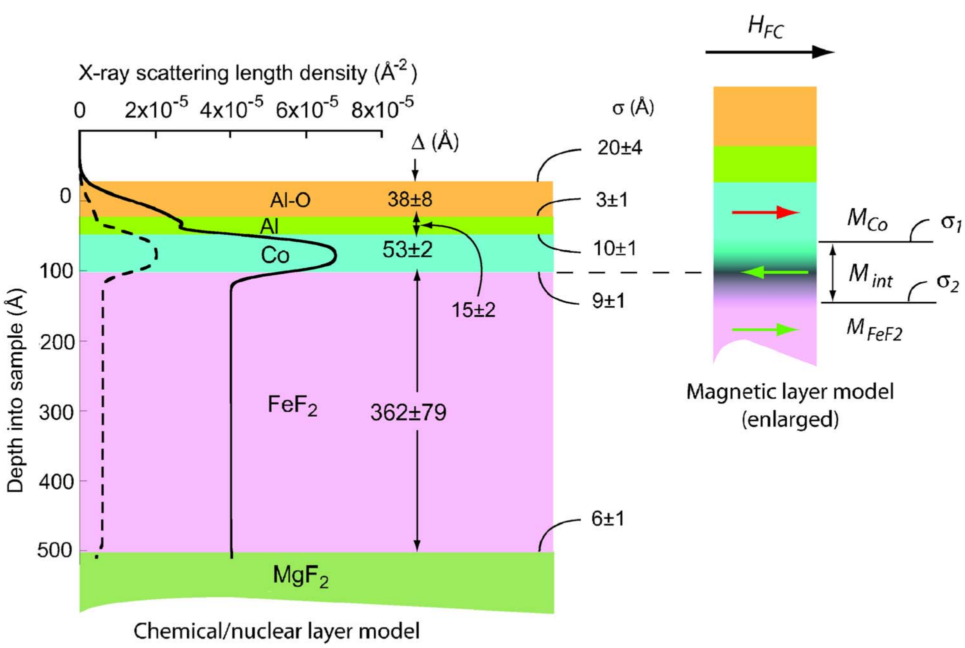

FIG. 2. (Color online) Left: The chemical/nuclear model structure showing the chemical layers, their thickness (Δ) and interface roughness (σ). The real (solid curve) and imaginary (dashed) components of the x-ray scattering length density are shown. Right: The scattering model is shown.

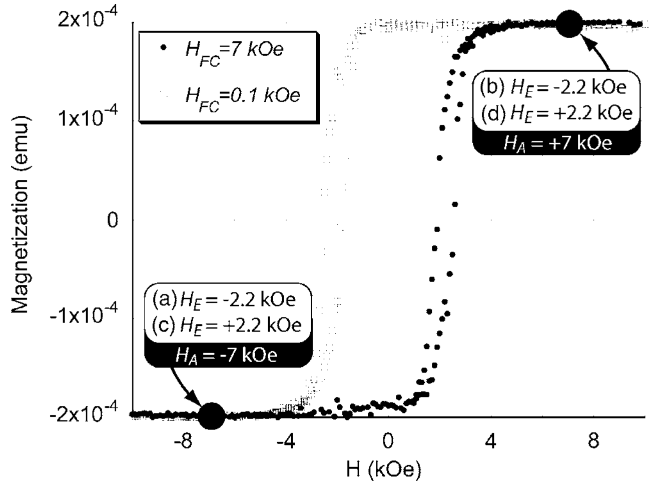

FIG. 3. Ferromagnetic hysteresis loops of the sample. The letters indicate the values of H_E and H_A corresponding to the neutron reflectivities in Fig. 4.

Neutron-scattering measurements were taken for $\pm H_E$ and $H_A = \pm 7$ kOe.[21] In each of these four configurations, two incident neutron beam polarizations (called up, i.e., neutron spin parallel to H_A, and down) were used. From a comparative analysis of the resulting four pairs of reflectivities (Fig. 4), the magnetization depth profiles can be separated into *pinned* and *unpinned* components (Appendix) for each sign of exchange bias.

After field cooling the sample to 10 K, H_A was cycled ±7 kOe three times—with the applied field of $H_A = +7$ kOe used for the neutron-scattering measurement. Positive applied field means that H_A and H_{FC} are parallel. The instrumental background corresponding to a reflectivity of order 10^{-7} has been removed. The data have been corrected for the nonperfect polarization of the neutron beam (polarization ~92%), the slightly imperfect flipping efficiency of the neutron flipper (~99.9+% efficient),[22,23] and the wavelength dependence of the neutron spectrum. The error bars in Figs. 4 and 5 include contributions associated with these corrections and the number of neutrons detected for each spin state and Q.

The two non-spin-flip reflectivities correspond to intensities measured for the same incident and reflected neutron beam polarizations, either both spin-up R^{++} or both spin-down R^{--}. The difference between R^{++} and R^{--} is related to the component of the net magnetization vector $\langle \vec{M}_\parallel \rangle$ parallel to $\vec{H}_A$ (Appendix). The averaging of $\vec{M}_\parallel$ to obtain $\langle \vec{M}_\parallel \rangle$ takes place over regions of the sample that scatter coherently—with a dimension we call the coherence dimension (typically microns in the sample plane).[24] The specular reflectivity is sensitive to the average of $\langle \vec{M}_\parallel \rangle$ within the coherence dimension. A nonzero value of $\langle \vec{M}_\parallel \rangle$ modulates the specular reflectivity with periods in Q that are inversely related to the thicknesses of the magnetic layers (Appendix). The difference between R^{++} and R^{--} is related to the strength of the magnetization (Appendix). For the case where magnetic domains form with dimensions smaller than the coherence dimension, $\langle \vec{M}_\parallel \rangle$ is reduced, and consequently, the difference between R^{++} and R^{--} is reduced. In addition, if the magnetizations of laterally separated domains are correlated, then off-specular diffuse (magnetic) scattering, where neutrons are reflected in directions other than specular, may be produced.[25] Because off-specular diffuse neutron scattering is very weak, studies have been limited to systems of patterned films[26–29] and multilayers of continuous films,[30] which are constructed to amplify the diffuse scattering signal, or confined to the region of reciprocal space near the critical edge,[31] where the specular reflectivity is close to unity. Spin dependence of off-specular neutron scattering is evidence for nonuniform laterally distributed magnetization, e.g., arising from domains, domain walls, and magnetic roughness. However, nonuniform laterally distributed magnetization is not a sufficient condition to produce off-specular scattering; for example, the lateral variations in the magnetization may not be correlated, or the correlation length may not be accessible for study with neutron reflectometry.[32] We found no spin-dependent off-

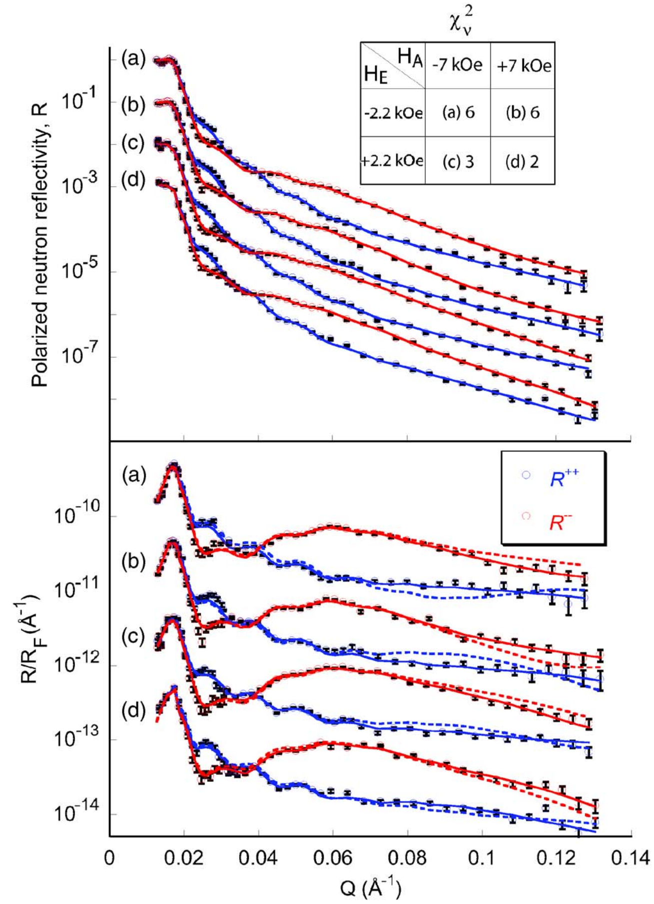

FIG. 4. (Color online) Upper panel: Observed (○) and calculated (solid curves) neutron reflectivities where each pair is labeled (a)–(d) according to the combinations of H_E and H_A corresponding to the conditions shown in Fig. 3 and those presented in the table of χ^2_ν (inset). Error bars are shown as black bars (for most data points much smaller than the symbols). Lower panel: The reflectivities times Q^4 are plotted versus Q. The solid curves are the reflectivities obtained from the magnetization depth profiles shown in Figs. 6 and 7. The dashed curves are the reflectivities calculated for a model having the *pinned* interfacial magnetization opposite to the directions shown in Fig. 8. Data are shifted for clarity.

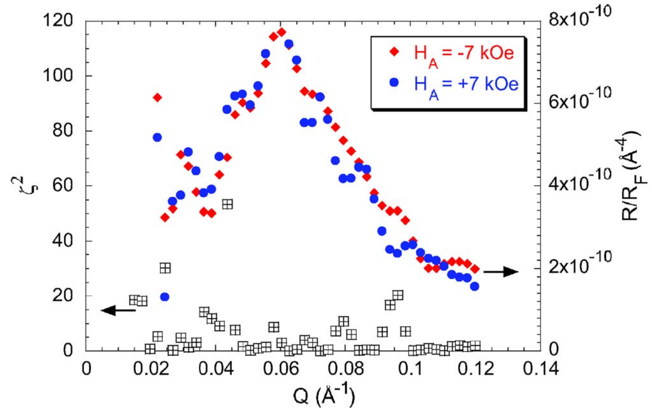

FIG. 5. (Color online) Plot showing quasiperiodic variation of $\zeta^2(Q)$ (open symbols) obtained from a comparison of the reflectivities taken for $H_A=\pm 7$ kOe and $H_E=-2.2$ kOe and spin-down incident neutron beam polarization. These reflectivities times Q^4 are shown as the closed symbols.

specular diffuse scattering either away from or near the critical edge (in contrast to observations in Ref. 31 of a different and much thicker magnetic system). For our system, diffuse scattering (of magnetic origin) is too weak to detect, or the dimensions of magnetic domains in our sample are not amenable for study with neutron reflectometry.

Qualitatively, the reflectivities (symbols in Fig. 4) (Ref. 33) for the same incident neutron beam polarization appear similar regardless of the orientation of H_A or the sign of H_E. To obtain a quantitative measure of the effect of H_A and H_E on the reflectivities, we evaluate $\zeta^2=\Sigma_i^{\nu}\frac{(R_{0i}-R_{1i})^2}{\Sigma_{0i}^2+\Sigma_{1i}^2}$, where $R_{0i}=R(s,H_A,H_E,Q_i)$ with standard deviation Σ_{0i} and $R_{1i}=R(s,H_A',H_E',Q_i)$ with standard deviation Σ_{1i} represent two data sets (reflectivities) and neutron spin states up (+) or down (−). Table I shows ζ_ν^2, i.e., ζ^2 normalized by the number of degrees of freedom ν [equal to the number of observations (45)]. ζ_ν^2 is generally much greater than 1, indicating that the difference between a pair of reflectivities having the same incident neutron beam polarization is larger than what can be attributed to random fluctuations of the data.[34] We show one such comparison in Fig. 5 for the pair of reflectivities corresponding to the conditions of $H_A=\pm 7$ kOe and $H_E=-2.2$ kOe. The quasiperiodic variation of $\zeta^2(Q)$ (Fig. 5) is a compelling evidence that differences between two reflectivities are not random. Since ζ_ν^2 is consistently greater than unity throughout Table I, we conclude that there are statistically significant differences between the reflectivities having different signs of H_E and H_A that warrant a quantitative analysis (model fitting).

The simplest exchange bias model treats the system as two magnetically distinct layers (e.g., FM and AF) coupled through an atomically sharp interface. However, more complex magnetic structures have been observed, including mixtures of ferromagnetic and antiferromagnetic exchange coupling,[7] domain walls perpendicular[13] and parallel[15] to the FM/AF interface, and inhomogeneity of magnetic anisotropy in the FM and AF layers.[35,36] Pertinent to our system are magneto-optical Kerr effect[37] measurements of similarly prepared samples. These measurements identified an incomplete

TABLE I. ζ_ν^2 for all possible combinations of reflectivity with the same incident neutron beam polarization but having different H_E and H_A. $\zeta_\nu^2\leq 1$ indicates statistically similar and $\zeta_\nu^2>1$ statistically different data sets.

	$H_E=-2.2$ kOe $H_A=+7$ kOe	$H_E=+2.2$ kOe $H_A=-7$ kOe	$H_E=+2.2$ kOe $H_A=+7$ kOe
		Spin down	
$H_E=-2.2$ kOe $H_A=-7$ kOe	6.5	31.5	22.1
$H_E=-2.2$ kOe $H_A=+7$ kOe		30.3	21.5
$H_E=+2.2$ kOe $H_A=-7$ kOe			1.8
		Spin up	
$H_E=-2.2$ kOe $H_A=-7$ kOe	4.0	6.4	4.4
$H_E=-2.2$ kOe $H_A=+7$ kOe		7.8	5.6
$H_E=+2.2$ kOe $H_A=-7$ kOe			1.8

domain wall (i.e., a domain wall with a twist less than 180°) parallel to the FM/AF interface when a strong field was applied opposite to H_{FC} for $-H_E$ (or parallel to H_{FC} for $+H_E$).

In order to allow for complex magnetic structures, we generated magnetization depth profiles using a scattering model consisting of three different magnetic layers corresponding to the FM, interface (int) region, and AF. The spin-dependent neutron specular reflectivity was calculated using the dynamical formalism of Parratt.[38] The process begins by choosing parameters for the scattering model, from which the spin-dependent neutron-scattering length density depth profiles $\rho(z)=\rho_n(z)\pm C'M(z)$, where $C'=2.853\times 10^{-9}$ Å^{-2} cm^3/emu, are calculated. The "+" ("−") sign is used for spin-up (down) incident neutron beam polarization. The parameters include the saturation magnetizations of each layer, M_{Co}, M_{int}, and M_{FeF2},[39] magnetic roughness σ_1 and σ_2 on either side of the interface region, and the thicknesses of the three layers (Fig. 2).

We imposed several constraints on the scattering model. Since the nuclear scattering length density depth profile of the sample is not affected by H_A or H_{FC}, it was constrained to be the same for all refinements. Second, the nuclear layer thickness and interface (chemical) roughness were optimized subject to the constraint that the optimal values lie within ranges shown in Fig. 2.[40] Third, M_{Co} was constrained to be the same for all refinements. Fourth, the sum of the magnetic thickness of the Co layer and the magnetic thickness of the interfacial region on the Co side of the Co/FeF_2 chemical interface was equal to the nuclear thickness of the Co layer. Fifth, the sum of the magnetic thickness of the interfacial region on the FeF_2 side of the Co/FeF_2 chemical interface and the magnetic thickness of the FeF_2 layer was equal to the nuclear thickness of the FeF_2 layer. Finally, the uncompensated magnetization in the bulk of the FeF_2 layer M_{FeF2} was constrained to be *pinned* as determined by Roy *et al.*[15] These

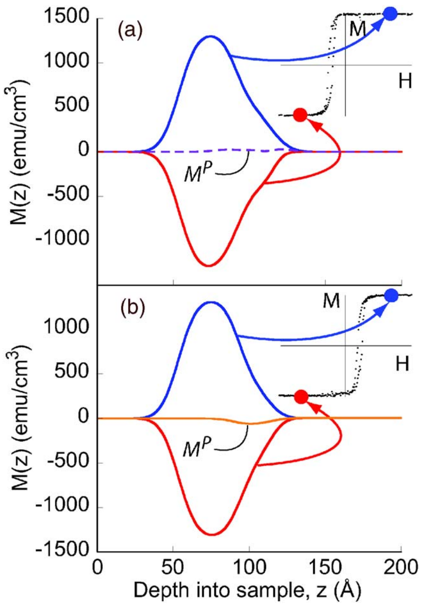

FIG. 6. (Color online) Net magnetization depth profiles for $H_A = +7$ kOe (blue curve) and $H_A = -7$ kOe (red curve) and (a) $H_E = -2.2$ kOe and (b) $H_E = +2.2$ kOe. The *pinned* components of the magnetization depth profiles are shown as the dashed purple and orange curves and in greater detail in Fig. 7(a).

constraints allow the interfacial region to have a magnetization depth profile containing *pinned* and *unpinned* components that may differ (though need not) from those of the adjoining layers, while preserving the chemical depth profile determined by x-ray reflectometry. The parameters were perturbed to minimize a measure of error χ^2 between the calculated and observed reflectivities using the Powell optimization procedure.[41] The calculated reflectivities that best fit the data are shown as solid curves in Fig. 4 and the magnetization in Fig. 6.

The projection of the *pinned* magnetization depth profiles along [001] FeF_2 for $\pm H_E$ can be obtained by determining the fractions of the magnetization depth profiles that do not change when H_A is reversed. If the magnetization depth profile $M(z)$ is composed of *pinned* and *unpinned* components, $M^P(z)$ and $M^U(z)$, respectively, then $M(\pm H_A, z) = M^P(z) \pm |M^U(z)|$, where $M(z)$ is shown as the red $(-H_A)$ and blue $(+H_A)$ curves in Fig. 6, and $M^U(-H_A, z) = -M^U(+H_A, z)$ is assumed. Solving for $M^P(z)$ and $M^U(z)$ yields

$$M^P(z) = \frac{1}{2}[M(+H_A,z) + M(-H_A,z)],$$

$$M^U(z) = \frac{1}{2}[M(+H_A,z) - M(-H_A,z)]. \quad (1)$$

$M^P(z)$ is plotted for the cases of $+H_E$ (orange) in Fig. 6(a) and $-H_E$ (dashed purple) in Fig. 6(b) and in much greater detail in Fig. 7(a). $M^U(z)$ is shown in Fig. 7(b) for $+H_E$ (orange) and $-H_E$ (dashed purple).

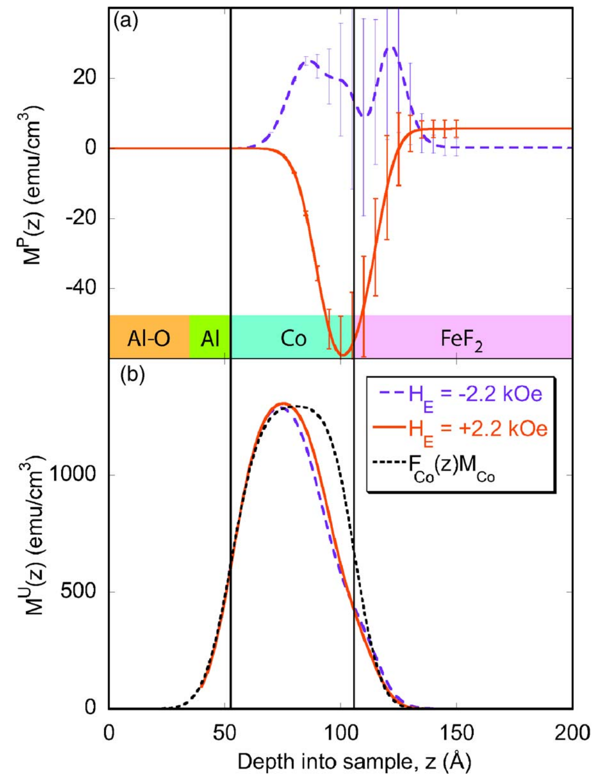

FIG. 7. (Color online) (a) *Pinned* and (b) *unpinned* magnetization depth profiles are shown for the cases of $H_E = -2.2$ kOe (dashed curve) and $H_E = +2.2$ kOe (solid curve). The short-dashed curve represents the product of the depth profile of the fraction of Co atoms F_{Co} and M_{Co}. The vertical lines are located at the centers of the Al/Co and Co/FeF_2 chemical interfaces.

IV. DISCUSSION OF THE MAGNETIZATION DEPTH PROFILE

There is a strong correlation relating the direction of the *pinned* magnetization with the sign of exchange bias. For $-H_E$, the *pinned* interfacial magnetization is parallel to H_{FC} (dashed purple curve, Fig. 7). For $+H_E$, the *pinned* interfacial magnetization is opposite to H_{FC} (orange curve, Fig. 7). The alignments of *unpinned* and *pinned* magnetizations are shown by red and green arrows, respectively, for cases of $-H_E$ (upper panel) and $+H_E$ (lower panel), and $-H_A$ (left) and $+H_A$ (right) relative to H_{FC} in Fig. 8. We find no evidence for a net *pinned* magnetization in the bulk of the AF for $-H_E$. In contrast, a net *pinned* magnetization parallel to H_{FC} is observed in the AF bulk for $+H_E$, which is consistent with Roy *et al.*[15]

The orientation of the *pinned* interfacial magnetization is contrary to the expectation based on the assumption of antiferromagnetic exchange coupling across an atomically sharp interface between *unpinned* moments in the FM and *pinned* moments in the AF. Specifically, the expected orientation is one with the green arrows corresponding to the interfacial magnetization in Fig. 8 reversed. In order to check whether the neutron data are truly sensitive to the orientation of the *pinned* interfacial magnetization, we repeated the refinement process constraining the *pinned* interfacial magnetization to be reversed from the orientation shown in Fig. 8. The best

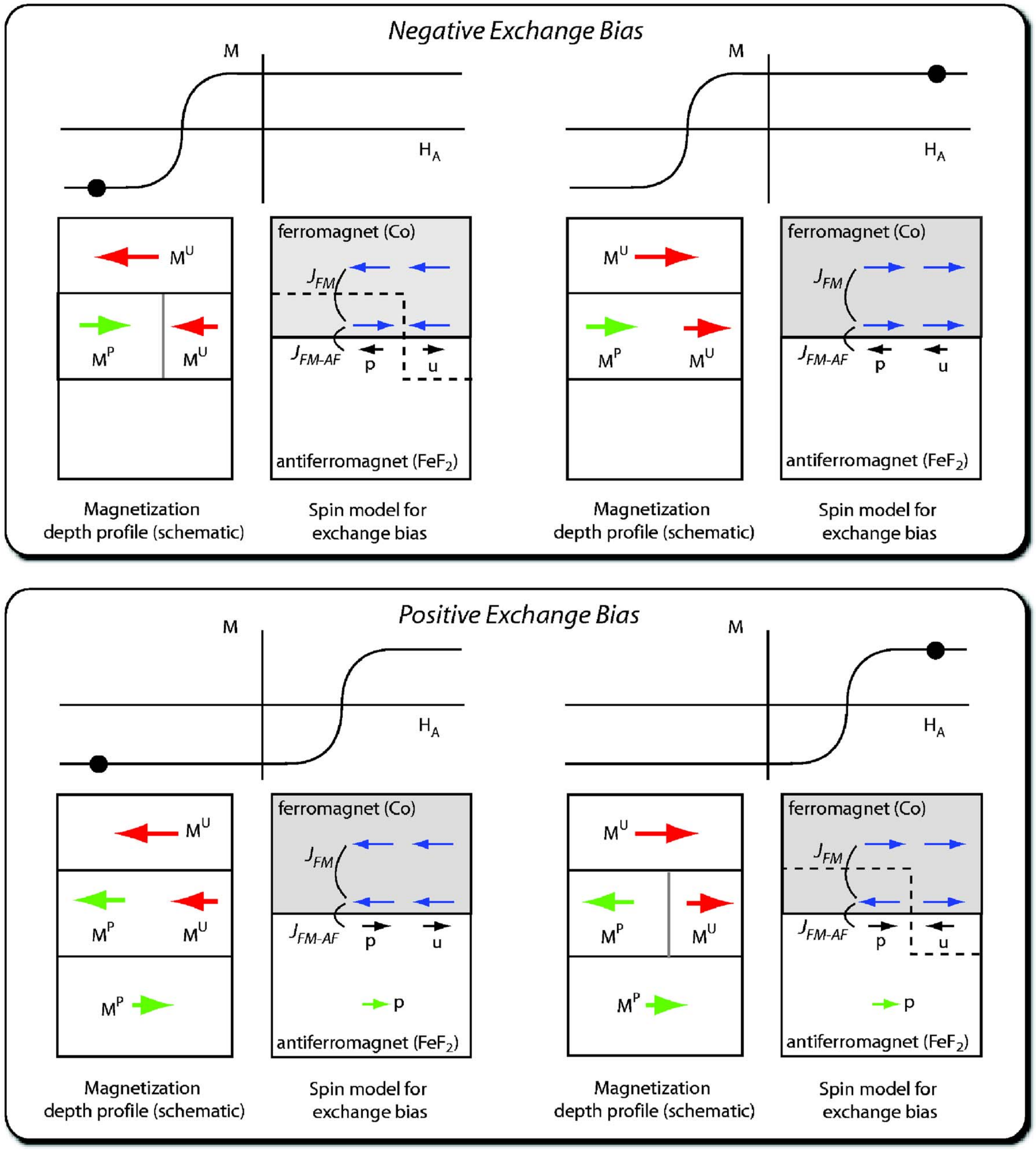

FIG. 8. (Color online) Schematic diagrams showing the configurations of the *pinned* and *unpinned* magnetization depth profiles obtained from Figs 6 and 7 corresponding to-$-H_E$ (upper panel) and $+H_E$ (lower panel). H_{FC} was applied parallel to $+|H_A|$. To the right of each of magnetization-depth-profile schematic is the exchange bias model showing the orientations of FM (Co) moments (blue arrows) and uncompensated AF (Fe) moments (black arrows) whose net moments yield the magnetization shown to the left. AF moments are identified as *pinned* or *unpinned* by the letters "p" and "u," respectively. FM moments that are coupled to pinned AF moments are effectively pinned.

fitting reflectivities are shown as the dashed curves in the lower panel of Fig. 4. The disagreement between the dashed curves and the neutron data is so compelling that a model for the *pinned* interfacial magnetization being opposite to H_{FC} for $-H_E$ and parallel to H_{FC} for $+H_E$ can be rejected.

Our analysis shows that the magnetic interface has a thickness larger than that attributable to chemical roughness. This implies the existence of *pinned* moments in the FM layer and not just in the AF layer as commonly assumed—a realization that hints towards the presence of domain walls that extend from the interface into the FM and/or AF.

For $-H_E$, the full width at half maximum (FWHM) of the *pinned* interfacial magnetization depth profile is 52 ± 2 Å and extends 27 ± 1 Å into the Co layer and 25 ± 1 Å into the FeF_2 layer relative to the chemical position of the Co/FeF_2 interface (at 53 ± 2 Å from the Co/Al interface).[42] The average of the *pinned* magnetization in the interfacial region is $\langle M^P_{\mathrm{int}}\rangle = 20\pm3$ emu/cm^3 (for $-H_E$). In the same region, the *unpinned* magnetization is $\langle M^U_{\mathrm{int}}\rangle = 575\pm16$ emu/cm^3. The ratio of $\langle M^P_{\mathrm{int}}\rangle$ to the sum of $\langle M^P_{\mathrm{int}}\rangle + \langle M^U_{\mathrm{int}}\rangle$ is the fraction $f^P_{-H_E} = 3.4\% \pm 0.6\%$ of *pinned* magnetization to the total magnetization in the interfacial region for $-H_E$.

TABLE II. Magnetization and areal moment density for $\pm H_E$. The "+" ("−") sign of the magnetization or areal moment density indicates that the quantity is parallel (antiparallel) to the cooling field.

Measurement	For $-H_E$	For $+H_E$
Co magnetization M_{Co} (emu/cm^3)	1299 ± 30	1299 ± 30
Magnetic interface width FWHM (nm)	5.2	2.7
Pinned interfacial magnetization $\langle M^P_{int} \rangle$ (emu/cm^3)	20 ± 3	-47 ± 3
Unpinned interfacial magnetization $\langle M^U_{int} \rangle$ (emu/cm^3)	575 ± 16	601 ± 14
FeF_2 bulk *pinned* magnetization $\langle M^P_{FeF_2} \rangle$ (emu/cm^3)	0 ± 2.5	5.6 ± 2.5
Percent *pinned* interfacial magnetization compared to the total interfacial magnetization, $f^P_{\pm H_E} = \frac{\lvert \langle M^P_{int} \rangle \rvert}{\lvert \langle M^P_{int} \rangle \rvert + \langle M^U_{int} \rangle} (\%)$	3.4 ± 0.6	7.3 ± 0.5
Unpinned areal moment density m^U (emu/cm^2)	$(6.08 \pm 0.14) \times 10^{-4}$	$(6.18 \pm 0.14) \times 10^{-4}$
Pinned interfacial areal moment density m^P_{int} (emu/cm^2)	$+(1.2 \pm 0.2) \times 10^{-5}$	$-(1.6 \pm 0.1) \times 10^{-5}$
Pinned areal moment density of the FeF_2 layer $m^P_{FeF_2}$(emu/cm^2)	$(0 \pm 0.1) \times 10^{-5}$	$+(2.1 \pm 0.1) \times 10^{-5}$
Sum of *pinned* areal moment densities $m^P = m^P_{int} + m^P_{FeF_2}$ (emu/cm^2)	$+(1.2 \pm 0.2) \times 10^{-5}$	$+(0.5 \pm 0.2) \times 10^{-5}$
Percent vertical shift of the hysteresis loop (as would be obtained by magnetometry), $\frac{m^P}{m^U + \lvert m^P \rvert} (\%)$	$+1.9 \pm 0.3$	$+0.8 \pm 0.3$

The areal moment density is the magnetization depth profile $M(z)$ integrated over the entire sample, e.g., $m^P = \int_{-\infty}^{\infty} M^P(z) dz$ (Table II).[43] The ratio of the *pinned* interfacial areal moment density m^P_{int} to the areal moment density of the whole sample is related to a vertical shift of the ferromagnetic hysteresis loop. Since the *pinned* areal moment density is positive, i.e., its direction is parallel to H_{FC}, an upward shift of the hysteresis loop (measured with magnetometry) along the vertical axis corresponding to $1.9\% \pm 0.3\%$ of M_{Co} is expected for $-H_E$. For small H_{FC}, such as that used to establish $-H_E$ for our sample, Nogués *et al.*[7] found upward or downward shifts of the hysteresis loop, depending on the sample.

For $+H_E$, the *pinned* interfacial magnetization is more tightly confined near the chemical Co/FeF_2 interface than for $-H_E$, and a net *pinned* magnetization is present in the bulk of the FeF_2 layer. The FWHM of the *pinned* interfacial magnetization is 27 ± 2 Å wide and extends 16 ± 1 Å into the Co layer and 11 ± 1 Å into the FeF_2 layer. As for the case of $-H_E$, the center of mass of the *pinned* interfacial magnetization for $+H_E$ is shifted somewhat towards the Co side of the chemical Co/FeF_2 interface. The mean value of the *pinned* interfacial magnetization is $\langle M^P_{int} \rangle = -47 \pm 3$emu/cm^3 (the negative sign indicates that the magnetization is opposite to H_{FC}) for $+H_E$. The *unpinned* magnetization in the same region is $\langle M^U_{int} \rangle = 601 \pm 14$ emu/cm^3. The fraction of *pinned* interfacial magnetization for $+H_E$ is $f^P_{+H_E} = 7.3 \pm 0.5\%$—slightly more than twice that found for $-H_E$.

The point where the *pinned* magnetization reverses sign for $+H_E$ is 21 ± 2 Å below the chemical Co/FeF_2 interface (i.e., inside the FeF_2 layer and ~ 125 Å from the sample's surface). The extension of the *pinned* interfacial magnetization into the FeF_2 layer is in the range of 20 to 35 Å previously identified from our x-ray and neutron-scattering studies.[15] If we attribute the *pinned* magnetization above the depth of 125 Å to the interfacial region and that below this depth to the FeF_2 layer, we obtain areal moment densities of $m^P_{int} = \int_{-125}^{\infty} M^P(z) dz = (-1.6 \pm 0.1) \times 10^{-5}$ emu/cm^2 for the interfacial region and $m^P_{FeF_2} = \int_{-\infty}^{-125} M^P(z) dz = (2.1 \pm 0.1) \times 10^{-5}$ emu/cm^2 for the bulk of the FeF_2 layer. A negative areal moment density is opposite to H_{FC}.

The interfacial areal moment density m^P_{int} is the number of *pinned* interfacial moments projected onto a plane per unit area. The fraction of *pinned* magnetization in the interfacial region compared to the total magnetization of the interfacial region is f^P. Our sample is one with an exchange bias of equal magnitude regardless of its sign, i.e., $\lvert -H_E \rvert = +H_E$. If exchange bias results from *pinned* interfacial moments, we conclude that $\lvert H_E \rvert$ is more closely related to the areal moment density than to the fraction of *pinned* interfacial magnetization since $\lvert m^P_{int}(-H_E) \rvert \approx \lvert m^P_{int}(+H_E) \rvert$, whereas $f^P_{+H_E} \approx 2 f^P_{-H_E}$.[44] Had the thickness of the interfacial region been the same for $\pm H_E$, then the fraction of *pinned* interfacial magnetization would have been the same, too.

The *pinned* areal moment density for the whole $+H_E$ sample is slightly positive $m^P = m^P_{int} + m^P_{FeF_2} = (0.5 \pm 0.2)$

$\times 10^{-5}$ emu/cm^2. Using this value and that of the *unpinned* areal moment density $m^U=(6.18\pm0.14)\times10^{-4}$ emu/cm^2, we expect an upward shift of the hysteresis loop along the vertical axis of $0.8\%\pm0.3\%$ of M_{Co} for $+H_E$. The upward shift of the hysteresis loop is somewhat less than for the case of $-H_E$ because the *pinned* interfacial areal moment density partially cancels that of the FeF_2 layer. Note that upward shifts of the hysteresis loops are expected regardless of the sign of exchange bias for this sample; thus, the sign of exchange coupling across the Co/FeF_2 interface cannot be inferred from a vertical shift of the hysteresis loop. It is noteworthy that the conclusions of Nogués *et al.*[7] are based on the assumption that *pinned* moments are located only at the interface. Hence, that model does not capture the effects that are attributed to the difference between the *pinned* moments in the interfacial layer and those in the FeF_2 bulk.[45,46] More generally, *pinned* uncompensated magnetization in the bulk of an antiferromagnet (or a ferrimagnet) may dominate the vertical shift of the hysteresis loop; thus, the sign of exchange coupling across the FM/AF interface cannot be determined from the sign of the vertical shift of a hysteresis loop with magnetometry.

The absolute value of the gradient of $M^U(z)$ is larger (i.e., steeper) on the Al side of the Co layer compared to that on the FeF_2 side of the Co layer [Fig. 7(b)]. To understand the asymmetry, we compare $M^U(z)$ to the profile that corresponds to the chemical variation of the Co number density profile (obtained from x-ray reflectometry). The fraction of the sample composed of Co as a function of depth into the sample $F_{\mathrm{Co}}(z)$ is calculated using

$$F_{\mathrm{Co}}(z)=\begin{cases}\dfrac{1}{2}\left[1+erf\left(\dfrac{z-\Delta_{\mathrm{Al/Co}}}{\sqrt{2}\sigma_{\mathrm{Al/Co}}}\right)\right] & z<\Delta_0\\[2ex] \dfrac{1}{2}\left[1-erf\left(\dfrac{z-\Delta_{\mathrm{Co/FeF2}}}{\sqrt{2}\sigma_{\mathrm{Co/FeF2}}}\right)\right] & z>\Delta_0,\end{cases} \tag{2}$$

where $\Delta_{\mathrm{Al/Co}}$ and $\Delta_{\mathrm{Co/FeF2}}$ are the positions of the interfaces, $\Delta_0=\Delta_{\mathrm{Al/Co}}+\Delta_{\mathrm{Co/FeF2}}$, and $\sigma_{\mathrm{Al/Co}}$ and $\sigma_{\mathrm{Co/FeF2}}$ are the roughnesses of the interfaces (Fig. 2). The anticipated magnetization depth profile of the Co moments is the product $F_{\mathrm{Co}}(z)M_{\mathrm{Co}}$ [black-short-dashed curve in Fig. 7(b)]. Near the Co/FeF_2 interface, $F_{\mathrm{Co}}(z)M_{\mathrm{Co}}$ is considerably larger than $M^U(z)$ for $\pm H_E$. The missing magnetization near the Co/FeF_2 interface represents about 22% of the anticipated areal moment density of the Co layer. Suppression of interfacial magnetization (along H_A) might result from a number of reasons including (1) domains that form such that the net magnetization of Co is diminished[47] (2) the magnetization from *unpinned* uncompensated moments in the FeF_2 layer negating some of the magnetization from *unpinned* Co moments (through antiferromagnetic exchange coupling)[15] and (3) the magnetization that may be rotated away from the applied field, diminishing the projection of the magnetization along the applied field. Suppression of interface magnetization along the applied field is consistent with the previously identified loss of Co moment density near the Co/FeF_2 interface.[15]

V. MODEL FOR EXCHANGE BIAS

The magnetization depth profiles provide several important insights. First, the width of the *pinned* magnetization near the Co/FeF_2 (FM/AF) interface is considerably larger than its chemical width [52 ± 2 Å ($-H_E$) and 27 ± 2 Å ($+H_E$) compared to 9 ± 1 Å]. Second, for $\pm H_E$, the center of mass of interfacial *pinned* magnetization is on the Co side of the Co/FeF_2 interface rather than the FeF_2 side. Together, these observations suggest that the interfacial region of *pinned* magnetization is not only in the AF as generally assumed, but also in the FM. The existence of *pinned* moments in the FM implies the existence of incomplete domain walls that separate domains of *pinned* magnetization from *unpinned* magnetization. Additionally, the much larger width of the interfacial *pinned* magnetization compared to the chemical interface width (roughness) suggests a magnetic structure that is distinct from either the FM or AF and extends into both regions. Guided by these observations, we propose an exchange bias model that assumes

(1) FM moments that greatly outnumber uncompensated AF moments,[15]

(2) ferromagnetic exchange coupling, J_{FM}, between FM moments,

(3) antiferromagnetic exchange coupling, $J_{FM\text{-}AF}$, between FM and AF moments across the interface,[6,15]

(4) some uncompensated AF moments that couple to the rigid structure of compensated AF moments below T_N with a pinning field larger than H_A (these are *pinned* moments), and

(5) other uncompensated AF moments, particularly at the interface, that remain *unpinned* below T_N.[15,18]

Shown to the right of the magnetization-depth-profile schematics in Fig. 8 are complementary schematics of the spin model for exchange bias. The magnetization in the FM and AF layers are dominated by FM and uncompensated AF moments, respectively. Since the magnetic interface straddles portions of the FM and AF, and because there are more FM moments than uncompensated AF moments, the orientation of the interfacial magnetization is mostly determined by the FM. Thus, for $-H_E$, *pinned* FM (uncompensated AF) moments are parallel (antiparallel) to H_{FC} as expected when exchange coupling across the FM/AF interface is antiferromagnetic for $+H_E$. The key element of the exchange bias model is the presence of *pinned* and *unpinned* moments in the FM and AF. This element is in contrast to the classical exchange bias model, where the moments in the FM are fully *unpinned* and the moments in the AF are *pinned*.

Our exchange bias model is not only consistent with the neutron- and soft-x-ray[15] scattering studies but is also consistent with an important conclusion of Ohldag *et al.*[48] Based on x-ray circular and linear dichroism studies, where the total electron yield was measured from a Co/FeF_2 bilayer exhibiting large $-H_E$, Ohldag *et al.*[48] concluded that the coupling between *pinned* Fe (AF) moments and Co (FM) moments is *antiferromagnetic* below T_N. Thus, at remanence Co moments will be antiparallel to *pinned* Fe moments. In our model, FM moments are antiparallel to the *pinned* AF moments at remanence for $\pm H_E$.

The exchange bias model also explains why the same sample may exhibit $\pm H_E$ depending on the strength of H_{FC}. First, consider the case for $+H_E$. To achieve $+H_E$, strong H_{FC} is required. The field orients uncompensated moments in the AF layer and the moments in the FM layer parallel to H_{FC} (overcoming $J_{FM\text{-}AF}$ at room temperature). After cooling to low temperatures, some of the uncompensated AF moments[14] become *pinned* by coupling to the ordered AF moments. For fields that do not overcome (i.e., frustrate) $J_{FM\text{-}AF}$ at low temperature, FM moments that are (antiferromagnetically) exchange coupled to *pinned* AF moments will be effectively *pinned*, but in a direction opposite to the *pinned* AF moments. FM moments that are exchange coupled to *unpinned* AF moments will be *unpinned* and will point along H_A (because the FM moments outnumber the AF moments). The *unpinned* AF moments will align in the opposite direction due to antiferromagnetic exchange coupling with the *pinned* FM moments. As the field is reduced below H_E from positive saturation, ferromagnetic exchange coupling between the *unpinned* and *pinned* FM moments will cause the magnetization of the FM to reverse its direction. Thus, the magnetization of the FM layer is negative for $H_A < +H_E$, and the hysteresis loop is shifted in the direction of H_{FC} (yielding $+H_E$). Since the FM moments constitute the majority of the *pinned* and *unpinned* interfacial magnetization, this magnetization points opposite to the cooling field for $H_A < +H_E$. As the field is increased from negative saturation above $+H_E$, *unpinned* FM and *unpinned* AF moments rotate together to maintain an antiparallel relationship with the FM magnetization parallel to H_A for $H_A > +H_E$. Consequently, domain walls (dashed lines in Fig. 8) form between *pinned* and *unpinned* moments (for $H_A > +H_E$). Magnetic domains decrease the net magnetization along H_A of the FM moments in the vicinity of the FM/AF interface, as observed here and previously in suppression of the *unpinned* interfacial magnetization.[15] (Experimental evidence for domains in similarly prepared samples has been published in Refs. 13 and 37.) The key requirement to produce $+H_E$ is for the product $H_{FC}M_{AF}$ to be large during cooling, so that M_{AF} will be parallel to H_{FC} at the expense of $J_{FM\text{-}AF}$.

Now, consider the case for $-H_E$. To achieve $-H_E$, the sample is cooled in a field just large enough to keep the FM magnetization parallel to H_{FC}, but not large enough to frustrate $J_{FM\text{-}AF}$. Because H_{FC} is weak, the alignment of uncompensated AF moments in the bulk is not favored; thus, little net magnetization is induced in the AF bulk. However, some AF moments near the FM/AF interface are aligned opposite to H_{FC} due to antiferromagnetic exchange coupling between these moments and FM moments that are aligned parallel to H_{FC}. At low temperatures, some of the AF moments become *pinned in the same direction*. These moments effectively pin the adjacent FM moments in the direction of the cooling field. Thus, when H_{FC} is weak, exchange coupling between FM and AF moments and the domain state of the FM layer determine the domain state of the AF. Subsequently, if H_A is increased towards positive saturation, FM moments, *pinned* or *unpinned*, will be parallel to H_A, and the AF moments, *pinned* or *unpinned*, will be opposite H_A. For a strong negative field, *unpinned* FM moments (and *unpinned* AF moments) move to be parallel (or opposite) to the H_A. This behavior of the *unpinned* moments is similar to the case of $+H_E$ and strong positive fields, while the *pinned* FM and *pinned* AF moments remain fixed (in directions opposite to the case of $+H_E$).

Regardless of the sign of H_E, when a strong field is applied in the direction the hysteresis loop is shifted, domain walls form to accommodate the different directions of the *pinned* and *unpinned* moments (or magnetization) (Fig. 8). The work done in creating the domain walls is related to $|H_E|$. For our sample, the work to create domain walls and thereby to reverse the sample magnetization is independent of the sign of H_E.

In our exchange bias model, the direction of the *pinned* AF moments is correlated with the sign of H_E and anticorrelated with the direction of the *pinned* FM moments. The direction of *pinned* AF moments is determined by competition between H_{FC} and $J_{FM\text{-}AF}$, which favor *pinned* moments in the AF that are parallel or antiparallel to strong or weak cooling fields, respectively.

VI. CONCLUSIONS

Good depth resolution and the ability to probe all depths in the sample with comparable sensitivity are intrinsic to neutron scattering. These attributes allowed us to characterize the magnetization depth profile across a Co/FeF_2 bilayer as a function of the sign of exchange bias. The distribution of *pinned* magnetization across the interface is nonuniform and is correlated with the sign of exchange bias. The width of the interfacial magnetization exceeds the width of the chemical interface—extending between ~13 Å (for $+H_E$) and ~26 Å (for $-H_E$) away from the average chemical interface into the FM and AF layers. An exchange bias model that consistently explains all experimental data was proposed. In this model, the interfacial region of *pinned* magnetization is composed of both *pinned* Co and *pinned* Fe moments residing in the FM and AF layers, respectively. This arises from antiferromagnetic exchange coupling that pins the Co moments close to the interface to *pinned* Fe moments, thus making these Co moments unresponsive to modest applied magnetic fields.

ACKNOWLEDGMENTS

Discussions with K. Liu (UCD), R. Morales (UCSD), and R. Stamps (UWA) are gratefully acknowledged. This work was supported by the Office of Basic Energy Science, U.S. Department of Energy, BES-DMS, the University of California Campus Laboratory Collaborative program, and Laboratory Directed Research and Development program funds. This work has benefited from the use of the Lujan Neutron Scattering Center at LANSCE, which is funded by the Department of Energy's Office of Basic Energy Science. Los Alamos National Laboratory is operated by Los Alamos National Security LLC under DOE Contract No. DE-AC52-06NA25396.

APPENDIX

To see that the *unpinned* and *pinned*magnetization depth profiles can be obtained from the polarized neutron (or x-ray) reflectivities $R^{\pm\pm}(\pm H_A,Q)$, consider a uniformly magnetized film on a nonmagnetic substrate. Using the Born approximation,[49] the reflectivity is given by

$$R_{BA}^{\pm\pm}(Q) = \frac{16\pi^2}{Q^2}\left|\int_{-\infty}^{\infty} e^{iQz}\rho^{\pm\pm}(z)dz\right|^2, \tag{A1}$$

where $\rho^{\pm\pm}(z)$ is the neutron-spin-dependent scattering length density at a depth of z into the sample averaged over its lateral dimensions.[23,50] For a thin FM layer with a nuclear scattering length density of ρ_0 and magnetization M on a nonmagnetic substrate with nuclear scattering length density ρ_1, $\rho^{\pm\pm}(z)$ is

$$\rho^{\pm\pm}(z) = \begin{cases} \rho_0 \pm C'M, & 0 < z < \Delta \\ \rho_1, & z > \Delta \\ 0 & \text{otherwise}, \end{cases} \tag{A2}$$

where $C' = 2.853 \times 10^{-9}$ Å^{-2} cm^3/emu. Substituting Eq. (A2) into Eq. (A1), integrating to obtain $R_{BA}^{\pm\pm}$, and neglecting terms in the delta function (i.e., considering only $Q \neq 0$), we obtain

$$R_{BA}^{\pm}(H,Q) = R_F[\rho_0 - \rho_1 \pm C'M(H)]^2(1 - \cos Q\Delta), \tag{A3}$$

where $R_F = 16\pi^2/Q^4$. If we consider M, the projection of $\vec{M}$ onto the direction of H_A, to be composed of *pinned* (M^P) and *unpinned* (M^U) magnetization, then $M = M^P + M^U$. For applied fields of $\pm H_A$ that saturate the *unpinned* magnetization, $M(\pm H_A) = M^P \pm |M^U|$, Eq. (A3) becomes

$$R_{BA}^{+}(\pm H_A,Q) = R_F(\rho_0 - \rho_1 + C'M^P \pm C'|M^U|)^2(1 - \cos Q\Delta),$$

$$R_{BA}^{-}(\pm H_A,Q) = R_F(\rho_0 - \rho_1 - C'M^P \mp C'|M^U|)^2(1 - \cos Q\Delta). \tag{A4}$$

From measurements using one incident beam polarization and opposite applied field directions, only two quantities can be obtained: $|M^U|$ and one of $\rho_0 - \rho_1 + C'M^P$ or $\rho_0 - \rho_1 - C'M^P$. However, if measurements are made using both incident beam polarizations and opposite field directions, then $|M^U|$ and M^P can be obtained separately. Since complicated magnetization depth profiles can be represented by a sequence of arbitrarily thin uniform profiles, M^U and M^P can be separated in general. The primary motivation to use polarized neutron reflectometry is to obtain the magnetization depth profiles for systems that are not uniform.

Previously, we stated that the difference between the non-spin-flip reflectivities was related to the magnetization depth profile. To understand what is meant by "related," Eq. (A3) is rewritten as

$$R_{BA}^{+}(H,Q) - R_{BA}^{-}(H,Q) = 4R_F(\rho_0 - \rho_1)C'M(1 - \cos Q\Delta). \tag{A5}$$

The difference $R_{BA}^{+}(H,Q) - R_{BA}^{-}(H,Q)$ is proportional to the magnetization through terms that vary (oscillate) with Q. These terms are the Fourier components of the magnetization depth profile. Since the oscillatory term is always positive (for a uniform film), the sign of $R_{BA}^{+}(H,Q) - R_{BA}^{-}(H,Q)$ depends on the product of the signs of $\rho_0 - \rho_1$, i.e., the difference between the *nuclear* scattering length densities of the magnetic film and its substrate, and the magnetization M.[51] Thus, the sign of $R_{BA}^{+}(H,Q) - R_{BA}^{-}(H,Q)$ for a single Q is not necessarily indicative of the orientation of M relative to H_A. For example, the nuclear scattering length density of Co is about one-half that of FeF_2; therefore, for a uniformly magnetized Co film on FeF_2, $R_{BA}^{-}(H,Q) > R_{BA}^{+}(H,Q)$ for all Q. On the other hand, for the same Co film on Si, $R_{BA}^{+}(H,Q) > R_{BA}^{-}(H,Q)$ for all Q because $\rho_{Co} > \rho_{Si}$. Provided the sample is simple, and the sign of $\rho_0 - \rho_1$ is known, the orientation of M relative to H_A can be obtained from inspection of $R_{BA}^{\pm}(H,Q)$ for a single Q. However, in practice, the sample structure is usually complex (e.g., the magnetic film may be capped to prevent oxidation, the magnetization may not be uniform, etc.). For complex structures, the orientation of M relative to H_A is obtained from an analysis (e.g., through model fitting) of many measurements of Q, as we have shown for our sample.

---

[1] W. H. Meiklejohn and C. P. Bean, Phys. Rev. **105**, 904 (1957).
[2] J. Nogués and I. K. Schuller, J. Magn. Magn. Mater. **192**, 203 (1999).
[3] A. E. Berkowitz and K. Takano, J. Magn. Magn. Mater. **200**, 552 (1999).
[4] R. L. Stamps, J. Phys. D **33**, R247 (2000).
[5] M. Kiwi, J. Magn. Magn. Mater. **234**, 584 (2001).
[6] J. Nogués, D. Lederman, T. J. Moran, and I. K. Schuller, Phys. Rev. Lett. **76**, 4624 (1996).
[7] J. Nogués, C. Leighton, and I. K. Schuller, Phys. Rev. B **61**, 1315 (2000).
[8] X. Ke, M. S. Rzchowski, L. J. Belenky, and C. B. Eom, Appl. Phys. Lett. **84**, 5458 (2004).
[9] F. Canet, S. Mangin, C. Bellouard, and M. Piecuch, Europhys. Lett. **52**, 594 (2000).
[10] H. Shi, D. Lederman, N. R. Dilley, R. C. Black, J. Diedrichs, K. Jensen, and M. B. Simmonds, J. Appl. Phys. **93**, 8600 (2003).
[11] O. Petracic, Z. P. Li, I. V. Roshchin, M. Viret, R. Morales, X. Batlle, and I. K. Schuller, Appl. Phys. Lett. **87**, 222509 (2005).
[12] P. Miltényi, M. Gierlings, J. Keller, B. Beschoten, G. Guntheradt, U. Nowak, and K. D. Usadel, Phys. Rev. Lett. **84**, 4224 (2000).
[13] I. V. Roshchin, O. Petracic, R. Morales, Z. P. Li, X. Batlle, and I. K. Schuller, Europhys. Lett. **87**, 297 (2005).
[14] The source of the uncompensated AF moments may be due to interfacial inhomogeneities, defects, or piezomagnetism.
[15] S. Roy *et al.*, Phys. Rev. Lett. **95**, 047201 (2005).
[16] The x-ray scattering length densities for Al and Co are in close agreement with literature values. The x-ray scattering length density for FeF_2 is about 17% larger than anticipated. This error could be explained by a misalignment of the sample by 0.025°.

[17] By cooling the sample from room temperature to 150 K in a field of 7 kOe, we assure that the sample's magnetization remains saturated above the Néel temperature of FeF_2.

[18] G. P. Felcher, R. O. Hilleke, R. K. Crawford, J. Haumann, R. Kleb, and G. Ostrowski, Rev. Sci. Instrum. **58**, 609 (1987).

[19] C. F. Majkrzak, Physica B **221**, 342 (1996).

[20] M. R. Fitzsimmons, S. D. Bader, J. A. Borchers, G. P. Felcher, J. K. Furdyna, A. Hoffmann, J. B. Kortright, I. K. Schuller, T. C. Schulthess, S. K. Sinha, M. F. Toney, D. Weller, and S. Wolf, J. Magn. Magn. Mater. **271**, 103 (2004).

[21] 7 kOe is the largest field that can be applied by our electromagnet when it accommodates the cryostat.

[22] S. Park, M. R. Fitzsimmons, X. Y. Dong, B. D. Schultz, and C. J. Palmstrom, Phys. Rev. B **70**, 104406 (2004).

[23] M. R. Fitzsimmons and C. F. Majkrzak, in *Modern Techniques for Characterizing Magnetic Materials*, edited by Y. Zhu (Kluwer, Boston, 2005), pp. 107–152.

[24] R. M. Richardson, J. R. P. Webster, and A. Zarbakhsh, J. Appl. Crystallogr. **30**, 943 (1997).

[25] S. K. Sinha, E. B. Sirota, S. Garoff, and H. B. Stanley, Phys. Rev. B **38**, 2297 (1988).

[26] K. Temst, M. J. Van Bael, and H. Fritzsche, J. Magn. Magn. Mater. **226**, 1840 (2000).

[27] D. R. Lee, G. Srajer, M. R. Fitzsimmons, V. Metlushko, and S. K. Sinha, Appl. Phys. Lett. **82**, 82 (2001).

[28] K. Theis-Brohl, H. Zabel, J. McCord, and B. P. Topererg, Physica B **356**, 14 (2005).

[29] C.-P. Li, I. V. Roshchin, X. Batlle, M. Viret, F. Ott, and I. K. Schuller, J. Appl. Phys. **100**, 074318 (2006).

[30] B. Nickel, A. Ruhm, W. Donner, J. Major, H. Dosch, A. Schreyer, H. Zabel, and H. Humbolt, Rev. Sci. Instrum. **72**, 163 (2001).

[31] S. G. E. te Velthuis, A. Berger, G. P. Felcher, B. K. Hill, and E. D. Dahlberg, J. Appl. Phys. **87**, 5046 (2000).

[32] Indeed, in studies of patterned films, the dimensions of the patterning *have been chosen* to assure that off-specular scattering could be detected by neutron reflectometry.

[33] Four weeks of neutron beam time were required to measure the eight reflectivity curves with a mean statistical precision of 5%.

[34] W. H. Press, B. P. Flannery, S. A. Teukolsky, and W. T. Vetterling, *Numerical Recipes, The Art of Scientific Computing* (Cambridge University Press, Cambridge, 1986), p. 470.

[35] M. R. Fitzsimmons, P. Yashar, C. Leighton, I. K. Schuller, J. Nogues, C. F. Majkrzak, and J. Dura, Phys. Rev. Lett. **84**, 3986 (2000).

[36] I. N. Krivorotov, C. Leighton, J. Nogues, I. K. Schuller, and E. D. Dahlberg, Phys. Rev. B **65**, 100402 (2002).

[37] R. Morales, Z. P. Li, O. Petracic, X. Batlle, I. K. Schuller, J. Olamit, and K. Liu, Appl. Phys. Lett. **89**, 072504 (2006).

[38] L. G. Parratt, Phys. Rev. **95**, 359 (1954).

[39] M_{FeF_2} represents the uncompensated magnetization of the antiferromagnetic FeF_2 layer.

[40] For example, the optimal thickness of the Al layer determined by x-ray reflectometry was 15 ± 2 Å, whereas the optimal value determined from the neutron reflectivity analysis was 13 Å.

[41] W. H. Press, B. P. Flannery, S. A. Teukolsky, and W. T. Vetterling, *Numerical Recipes, The Art of Scientific Computing* (Cambridge University Press, Cambridge, 1986), p. 294.

[42] Errors on the spatial extent of the layers were determined from a statistical analysis of the fit to the neutron data. Sensitivity of the fit to fine details of the magnetization profile is limited by the finite range of Q over which the reflectivity was obtained. Averaging of the scattering amplitude occurs over lateral dimensions (tens of microns) related to the coherence of scattering and may further obscure fine details.

[43] The error in the *pinned* areal moment density was determined from the variation of the *pinned* magnetization depth profile, which was obtained from a statistical analysis of the fit to the neutron data.

[44] To define f^P, the peak value of M^P could have been used instead of $\langle M^P_{\text{int}}\rangle$. This approach yields larger values for $f^P_{+H_E}$ and $f^P_{-H_E}$ of $\sim$9% and $\sim$5%, respectively. The ratio of the two values is still about a factor of 2.

[45] J. Mattsson, C. Djurberg, and P. Norblad, J. Magn. Magn. Mater. **136**, L23 (1994).

[46] Ch. Binek, Xi Chen, A. Hochstrat, and W. Kleemann, J. Magn. Magn. Mater. **240**, 257 (2002).

[47] Z. P. Li, O. Petracic, R. Morales, J. Olamit X. Batlle, K. Liu, and I. K. Schuller, Phys. Rev. Lett. **96**, 217205 (2006).

[48] H. Ohldag, H. Shi, E. Arenholz, J. Stohr, and D. Lederman, Phys. Rev. Lett. **96**, 027203 (2006).

[49] When fitting models to reflectivity data the dynamical formalism (Ref. 38) was used.

[50] More precisely, the average is taken over the region of the sample which coherently scatters the neutron (or x-ray) beam.

[51] A similar situation is encountered with resonant soft-x-ray reflectometry which makes interpretation of the sign of coupling between two magnetic species difficult, if not impossible, to determine from simple inspection of hysteresis loops. However, the sign of the coupling can be determined from model fitting (e.g., see Ref. 15).